2011

An Optimal Current Control Strategy for a Three-Phase Grid-Connected Photovoltaic System Using Particle Swarm Optimization

Waleed Al-Saedi
Edith Cowan University

Stefan W. Lachowicz
Edith Cowan University

Daryoush Habibi
Edith Cowan University

An Optimal Current Control Strategy for a Three-Phase Grid-Connected Photovoltaic System Using Particle Swarm Optimization

Waleed Al-Saedi, Stefan W. Lachowicz, *Senior Member*, *IEEE*, and Daryoush Habibi, *Senior Member*, *IEEE*
School of Engineering, Edith Cowan University, Perth, Western Australia
Email: walsaedi@our.ecu.edu.au

***Abstract*—A robust current control strategy for PV (photovoltaic) grid-connected systems is required for reliable use of solar energy as an abundant and clean renewable energy. This paper presents real time optimization parameters of the current control strategy for a 3-phase photovoltaic grid-connected Voltage Source Inverter (VSI) system. The proposed controller scheme is implemented based on a synchronous reference frame; the Phase-Locked Loop (PLL) is used as grid phase detector. Particle Swarm Optimization (PSO) algorithm is an intelligent searching algorithm that is used to implement the real time self-tuning method for the current control parameters. Two conventional PI controllers are used and feed-forward compensation is applied with the inner inverter current control loop to achieve fast dynamic response. The main aim of this work is to achieve high dynamic response for the inverter output current with acceptable harmonics level in steady-state condition all of which is required for power quality improvement. The results show that the proposed strategy provides an excellent dynamic response within real time optimization.**

***Index Terms*—Grid-connected system, photovoltaic, current control, Particle Swarm Optimization (PSO).**

I. INTRODUCTION

The high penetration of renewable energy sources depends on promising alternative sources that provide green energy and flexible extension of the present electrical distribution network capacity [1]. Currently, Distributed Generation Units (DGs) such as photovoltaic, wind, hydro, fuel cell, and batteries represent the common green power sources. These sources usually need a power electronic converter unit to interface with the utility in order to form a grid connected system. Pulse-width-modulation (PWM) VSI systems are widely used in such systems. These applications have nonlinear voltage-current characteristics of semiconductor devices and exhibit increased switching frequency both of which affect the quality of the power supply [2].

In such systems, the current control strategy is responsible for providing the quality of power supply by which DG units are connected to the grid. The current error compensation and the PWM generation are the main two tasks for this application. There are two main categories for the current control strategy; nonlinear controllers based on closed loop current type PWM and linear controllers based on open loop voltage type PWM, and both are applied using the inner current feedback loop [3].

In the nonlinear controller, hysteresis current control (HCC) is commonly used for 3-phase grid-connected VSI system. The HCC unit compensates the current error and generates PWM signals with acceptable dynamic response. While the current is controlled independently with a control delay, zero voltage vectors cannot be generated thus providing large current ripples with high total harmonic distortion (THD) [4]. Conversely, linear current controller based space vector PWM (SVPWM) is an adequate controller that separates the current error compensation and PWM generation. This controller yields an excellent steady-state response, low current ripples, and good sinusoidal waveform. The current error is usually compensated either by proportional-integral (PI) regulator or predictive control algorithm. In addition, the SVPWM has many aspects that help to improve the control strategy such as constant switching frequency, optimum switching pattern, and excellent DC-link voltage utilization [5].

The mathematical model of a three-phase grid connected photovoltaic inverter is presented in [6]. The controller is implemented based on synchronous PI current regulator with the aim of describing the strategy of the controller and providing all the information needed for analysis and design. Furthermore, in [7] and [8], the SVPWM based PI current regulator was applied for 3-phase grid-connected photovoltaic and AC/DC converter models. System response was studied in these works but the process lacked automatic calculation of the control parameter tuning.

In this paper, linear current controller-based SVPWM is proposed for a three-phase PV grid-connected VSI model. The proposed controller scheme is implemented using synchronous reference frame. Two conventional PI controllers are used and feed-forward compensation is applied to the inner inverter current control loop to achieve high dynamic response. Particle Swarm Optimization (PSO) algorithm is considered for real time self-tuning parameters, with Integral Time Absolute Error (ITAE) as an objective function that calculates 1/3 Simpson's rule. The aim of this work is power quality improvement. The simulation results demonstrate that the controller provides an excellent dynamic response.

II. SYSTEM DESCRIPTION

A. PV array model

As shown in Figure 1, the solar cell can be described as a p-n junction. Hence, I_{ph} is the photo current proportional to the insolation $E(Kw/m^2)$, I_D is the diode current, I_p is parallel current, R_s is series resistor, R_p is parallel resistor, V_D is the diode voltage, and V_C is the cell voltage. The output current (I_C) can be expressed by equation (1) [1].

$$I_C = I_{ph} - I_D - I_p \tag{1}$$

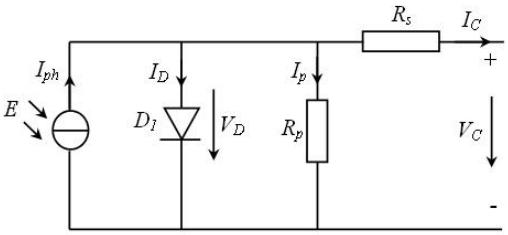

Figure 1. Equivalent circuit of a PV array

where;

$$\begin{cases} I_D = I_s.\left\{exp\left(\frac{V_D}{m.V_T}\right) - 1\right\} \\ V_D = V_C + I_C.R_s \\ V_T = \frac{k.T}{e} \\ I_p = \frac{V_D}{R_p} \end{cases} \tag{2}$$

and I_s is diode saturation current, V_T is thermal voltage, m is diode factor, k is Boltzmann constant $(1.38\times10^{-23}J/K)$, T is absolute temperature, and e is electron charge (1.6×10^{-19}) in Coulombs. Therefore, the output power of a PV array depends on the number of cells in series (N_s) and in parallel (N_p) in order to meet the required rated power. The overall voltage and current can be expressed as following equations, respectively:

$$V_{dc} = N_s(V_d - I_C R_S) \tag{3}$$

$$I_{dc} = N_p I_C \tag{4}$$

B. 3-phase grid-connected VSI model

A typical topology of a grid-connected VSI system is shown in Figure 2. In the abc reference frame, the state equations of the equivalent circuit are given by [9]:

$$\frac{d}{dt}\begin{bmatrix} i_a \\ i_b \\ i_c \end{bmatrix} = \frac{R_s}{L_s}\begin{bmatrix} i_a \\ i_b \\ i_c \end{bmatrix} + \frac{1}{L_s}\left(\begin{bmatrix} V_{sa} \\ V_{sb} \\ V_{sc} \end{bmatrix} - \begin{bmatrix} V_a \\ V_b \\ V_c \end{bmatrix}\right) \tag{5}$$

Using Park's transformation, equation (5) can be transformed into a d-q reference frame as the following equation:

$$\frac{d}{dt}\begin{bmatrix} i_d \\ i_q \end{bmatrix} = \begin{bmatrix} -\frac{R_s}{L_s} & \omega \\ -\omega & -\frac{R_s}{L_s} \end{bmatrix}\begin{bmatrix} i_d \\ i_q \end{bmatrix} + \frac{1}{L_s}\left(\begin{bmatrix} V_{sd} \\ V_{sq} \end{bmatrix} - \begin{bmatrix} V_d \\ V_q \end{bmatrix}\right) \tag{6}$$

where ω is grid angular frequency and the Park's transformation can be defined as:

$$i_{dq0} = T i_{abc} \tag{7}$$

where;

$$i_{dq0} = \begin{bmatrix} i_d \\ i_q \\ i_0 \end{bmatrix},\ i_{abc} = \begin{bmatrix} i_a \\ i_b \\ i_c \end{bmatrix} \tag{8}$$

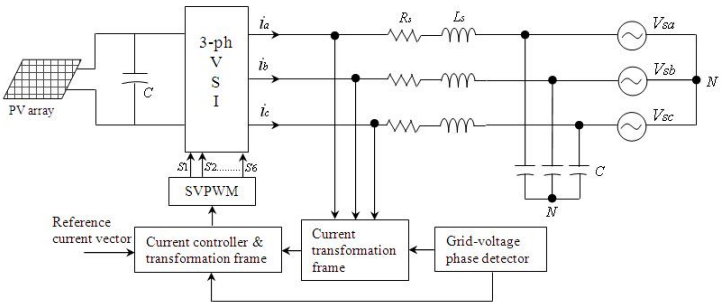

Figure 2. 3-phase grid-connected VSI model

$$T = \frac{2}{3}.\begin{bmatrix} cos\theta & cos(\theta - \frac{2\pi}{3}) & cos(\theta + \frac{2\pi}{3}) \\ -sin\theta & -sin(\theta - \frac{2\pi}{3}) & -sin(\theta + \frac{2\pi}{3}) \\ \frac{1}{2} & \frac{1}{2} & \frac{1}{2} \end{bmatrix} \tag{9}$$

$\theta = \omega_s t + \theta_o$ is the synchronous rotating angle. Consequently, the key characteristic of the current controller-based PI regulator that generates the reference voltage signals, can be given by:

$$\begin{bmatrix} V_d^* \\ V_q^* \end{bmatrix} = \begin{bmatrix} -K_p & -\omega L_s \\ \omega L_s & -K_p \end{bmatrix}\begin{bmatrix} i_d \\ i_q \end{bmatrix} + \begin{bmatrix} K_p & 0 \\ 0 & K_p \end{bmatrix}\begin{bmatrix} i_d^* \\ i_q^* \end{bmatrix} + \begin{bmatrix} K_i & 0 \\ 0 & K_i \end{bmatrix}\begin{bmatrix} X_d \\ X_q \end{bmatrix} + \begin{bmatrix} V_{sd} \\ V_{sq} \end{bmatrix} \tag{10}$$

where $\frac{dX_d}{dt} = i_d^* - i_d$ and $\frac{dX_q}{dt} = i_q^* - i_q$

III. CURRENT CONTROL STRATEGY

A. Control system configuration

As shown in Figure 3, the block diagram of the proposed current controller is designed based on a d-q synchronous rotating frame. Although the output current of the inverter and the grid voltage are transformed into a synchronous frame, it was necessary to use Phase-Locked Loop (PLL) to detect the grid voltage phase angle in order to implement Park's transformation in the control scheme. Two conventional PI regulators are used to eliminate current error. In this work, a PSO algorithm is implemented in order to tune PI parameters in real time operation to minimize the error between the inverter output current and the reference current provided from the output of the PV array. In addition, the feed-forward compensation of the grid voltage is applied to compensate the grid harmonics. Consequently, the output signals of the controller represent the reference voltage signals in the d-q frame, followed by the inverse d-q to abc transformation in order to generate six pulses by SVPWM to fire the Insulated-gate Bipolar Transistor (IGBT) inverter.

B. Particle Swarm Optimization (PSO) Algorithm

Particle Swarm Optimization (PSO) was proposed by Kennedy and Eberhart in 1995 [10]. It is an Evolutionary Computation (EC) technique that simulates the social behavior of the swarm in nature such as schools of fish or flocks

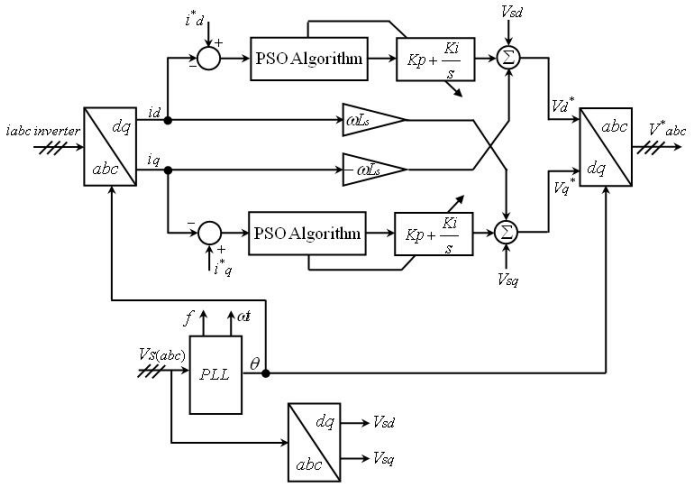

Figure 3. Current control scheme

of birds where they find food together in a specific area. More specifically, PSO is an iterative algorithm that depends on searching the space in order to determine the optimal solution of an objective function (fitness function) [11]. This algorithm's evaluation is based on the movement of each particle as well as collaboration of the swarm. Each particle starts to move randomly based on its own best knowledge and the swarm's experience. It is also attracted toward the location of current global best position X_{gbest} and its own best position X_{pbest}[12]. The basic rules of PSO algorithm can be described in three main stages:

1) Evaluating fitness value of each particle
2) Updating local and global best fitness and positions
3) Updating velocity and position of each particle

Mathematically, the search process can be expressed by simple equations regarding the position vector $X_i = [x_{i1}, x_{i2}, ..., x_{in}]$ and the velocity vector $V_i = [v_{i1}, v_{i2}, ..., v_{in}]$ in the specific dimensional search space. In addition, the optimality of the solution in PSO algorithm depends on each particle position and velocity update using the following expressions [13]:

$$V_i^{k+1} = w.V_i^k + c_1.r_1[X_{pbest}^k - X_i^k] + c_2.r_2[X_{gbest}^k - X_i^k] \quad (11)$$

$$X_i^{k+1} = X_i^k + V_i^{k+1} \quad (12)$$

where *i* is the index of the particle; V_i^k, X_i^k are the velocity and position of particle *i* at iteration *k,* respectively; w is the inertia constant set between [0 1]; c_1 and c_2 are coefficient factors often set to 2; r_1 and r_2 are random values between [0 1] that are generated for each velocity update; X_{gbest} and X_{pbest} are the global best position that is achieved so far, based on the swarm's experience, and local best position of each particle that is achieved so far, based on its own best position, respectively.

A confined search space is the main limitation of the PSO algorithm. Limited search space provides for the fast solution, but influence the optimality of the solution if the global optimum value is located outside the boundaries. However, extended boundaries allow finding global optimum results, but need more time to determine the global optimal value in the search space [9]. Therefore, more information about the limits of the parameters will help to determine the search boundaries. Figure 4 shows the flowchart of the implemented PSO algorithm.

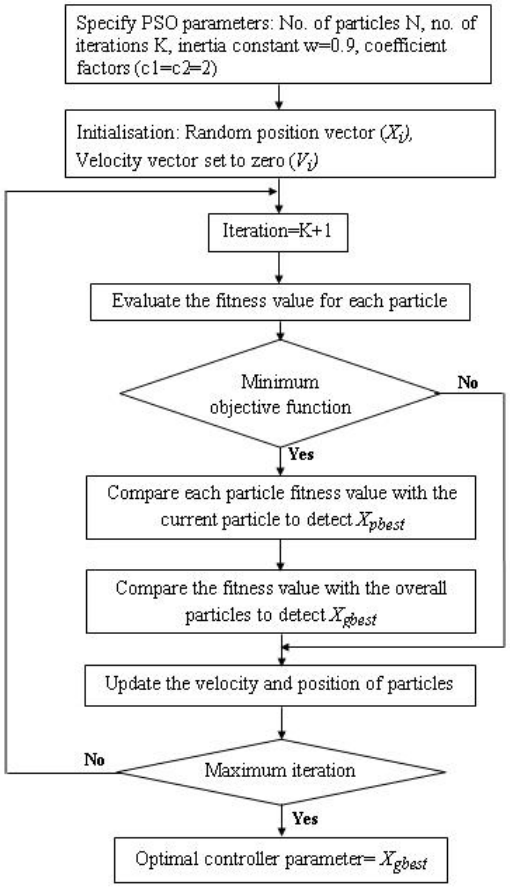

Figure 4. Flowchart of the applied PSO algorithm

C. Fitness Function

The fitness function is a particular type of the objective function that provides the optimality of the solution. Obviously, various objective functions can be used by the PSO algorithm. In this paper, the controller's fitness function is based on ITAE which is calculated using Simpson's 1/3 rule. The mathematical expression of the ITAE performance index is given by equation (13) [14]:

$$ITAE = \int_0^\infty t \mid e(t) \mid dt \quad (13)$$

where t is the time and $e(t)$ is the difference between the reference set point and the controlled signal.

D. Termination Criteria

In general, termination criteria of PSO algorithm can be considered either when the algorithm achieves the maximum

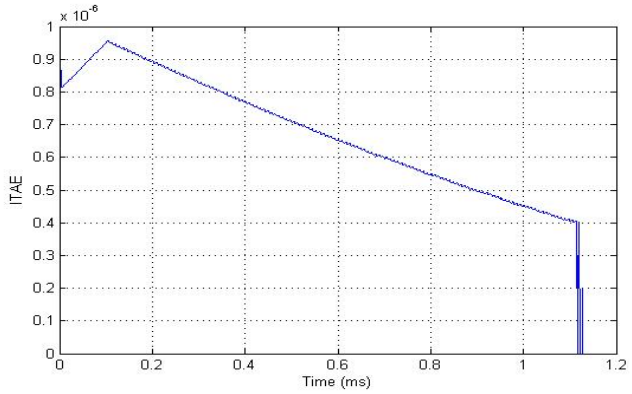

Figure 5. PSO search process

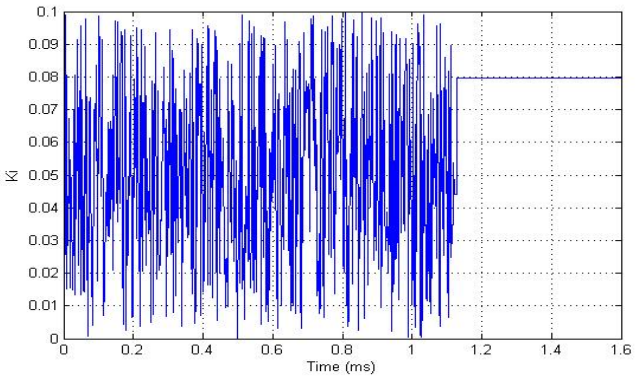

Figure 7. Best solutions of K_i for 100 iterations

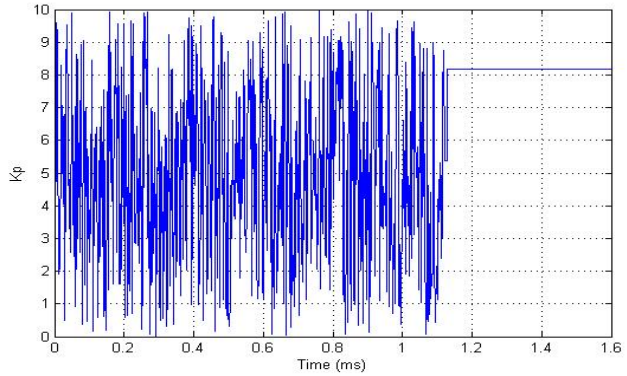

Figure 6. Best solutions of K_p for 100 iterations

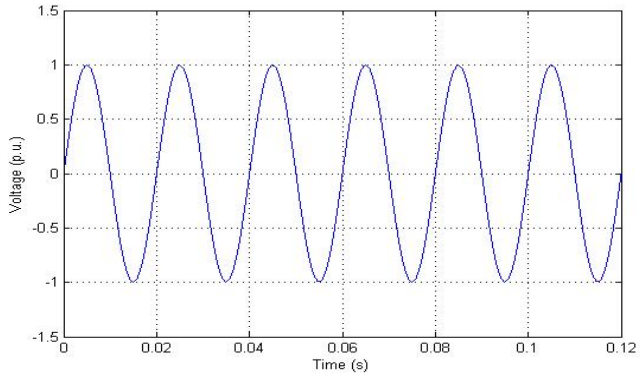

Figure 8. Simulation results of grid phase voltage

number of iterations or acceptable fitness value. In this work, the minimization of the objective function is considered with the maximum number of iterations to select the optimal parameter values for the two PI regulators. The result of the PSO search process is shown in Figure 5. It can be seen that the error value has decreased at the end of the iterations. Figures 6 and 7 show the trajectories of the particle's position (candidate solutions) for 100 iterations. The algorithm must find the best solution to provide the optimal values of the control parameters. In steady-state, the final optimal K_p and K_i parameters are 8.1659 and 0.0796, respectively.

IV. SIMULATION RESULTS

As shown in Figure 2, the control strategy of the 3-phase grid-connected VSI model is implemented using MATLAB/Simulink environment. PSO algorithm and its objective function are separately programmed by a MATLAB/M-file program. The model parameters are $L_s = 3$ mH, R_s=1.2 Ohm, f=50 Hz, and the input capacitor of the dc side is 100 μF. The output power of the PV array system is 510 W for six modules with the output DC voltage of 103.2 V. Insolation variations are considered from 0-1000 W/m^2. For the SVPWM-based current controller, switching and sampling frequency are fixed at 10 kHz and 500 kHz, respectively. An IGBT inverter type is used and all simulation results are in a p.u. system.

In order to verify the control performance, Figures 8 and 9 show the simulated steady-state response. It can be clearly seen that the grid phase voltage and line current waveforms are highly sinusoidal and maintain a steady state condition even when the insolation value has been changed during operation. The dynamic response of current controller is evaluated in this work as depicted in Figures 10 and 11. At 0.12 seconds the reference current is stepped and after this time the inverter is operating in steady state condition. Overall, the controller provides an excellent dynamic response.

Figure 12 shows the spectrum of the simulation waveform of the line current. The results verify that the proposed control strategy compensates current harmonic distortion effectively. The total harmonic distortion (THD) is 0.38% which is well below the 5% THD allowed in IEEE Std 1547-2003 [15].

V. CONCLUSION

In this paper, a linear current controller-based SVPWM has been proposed for a three-phase PV grid-connected VSI model. The proposed controller scheme was implemented based on synchronous reference frame, using two conventional PI controllers and applying feed-forward compensation with the inner inverter current control loop to achieve high dynamic response. PSO was used for real time self-tuning parameters, and ITAE was used as an objective function that was calculated using Simpson's 1/3 rule. Power quality improvement was the objective of this work, and the simulation results have shown that the proposed controller offers an excellent dynamic response.

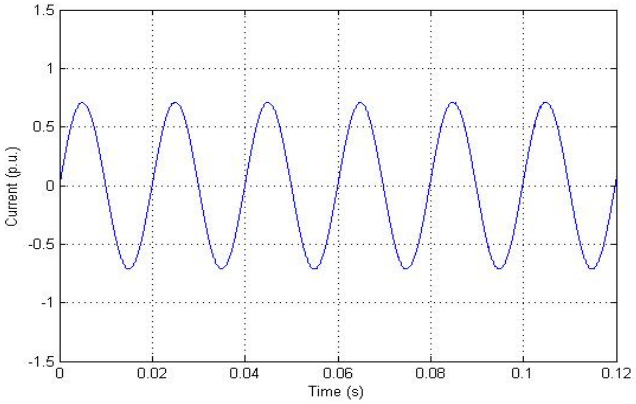

Figure 9. Simulation results of line current at steady-state condition

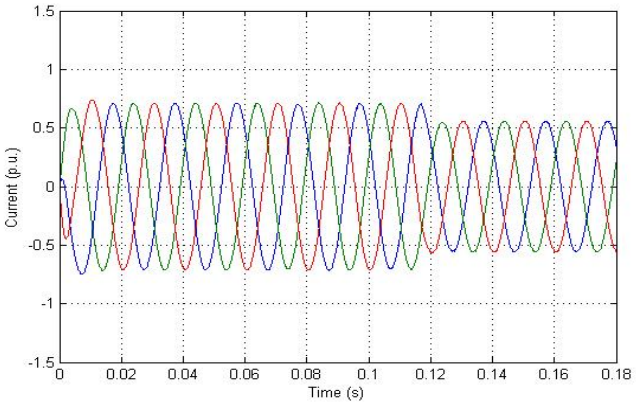

Figure 10. System dynamic response of the step-down at 0.12 seconds

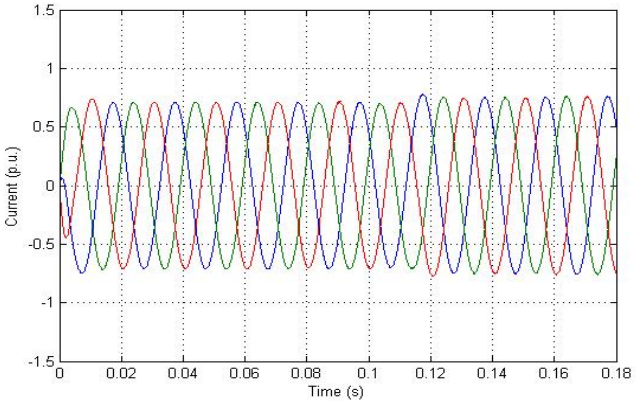

Figure 11. System dynamic response of the step-up at 0.12 seconds

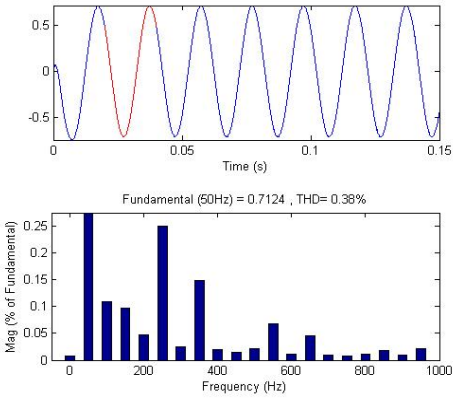

Figure 12. Spectrum of the grid phase current

REFERENCES

[1] R.Strzelecki and G.Benysek, *Power electronics in smart electrical energy networks*. Verlag London: Springer, 2008.

[2] D. Menniti, A. Burgio, A. Pinnarelli, and N. Sorrentino, "Grid-interfacing active power filters to improve the power quality in a microgrid," in *Harmonics and Quality of Power, 2008. ICHQP 2008. 13th International Conference on*, pp. 1–6.

[3] Z. Qingrong and C. Liuchen, "Study of advanced current control strategies for three-phase grid-connected pwm inverters for distributed generation," in *Control Applications, 2005. CCA 2005. Proceedings of 2005 IEEE Conference on*, pp. 1311–1316.

[4] K. Bong-Hwan, M. Byung-Duk, and Y. Jang-Hyoun, "An improved space-vector-based hysteresis current controller," *Industrial Electronics, IEEE Transactions on*, vol. 45, no. 5, pp. 752–760, 1998.

[5] M. P. Kazmierkowski and L. Malesani, "Current control techniques for three-phase voltage-source pwm converters: a survey," *Industrial Electronics, IEEE Transactions on*, vol. 45, no. 5, pp. 691–703, 1998.

[6] M. Liang, R. Wang, and T. Q. Zheng, "Modeling and control of three-phase grid-connected photovoltaic inverter," in *Control and Automation (ICCA), 2010 8th IEEE International Conference on*, pp. 2240–2245.

[7] Z. Hui, Z. Hongwei, R. Jing, L. Weizeng, R. Shaohua, and G. Yongjun, "Three-phase grid-connected photovoltaic system with svpwm current controller," in *Power Electronics and Motion Control Conference, 2009. IPEMC '09. IEEE 6th International*, pp. 2161–2164.

[8] J. W. G. Hwang, M. Winkelnkemper, and P. W. Lehn, "Design of an optimal stationary frame controller for grid connected ac-dc converters," in *IEEE Industrial Electronics, IECON 2006 - 32nd Annual Conference on*, pp. 167–172.

[9] C. Il-Yop, L. Wenxin, D. A. Cartes, and K. Schoder, "Control parameter optimization for a microgrid system using particle swarm optimization," in *Sustainable Energy Technologies, 2008. ICSET 2008. IEEE International Conference on*, pp. 837–842.

[10] J. Robinson and Y. Rahmat-Samii, "Particle swarm optimization in electromagnetics," *Antennas and Propagation, IEEE Transactions on*, vol. 52, no. 2, pp. 397–407, 2004.

[11] J. Kennedy and R. Eberhart, "Particle swarm optimization," in *Neural Networks, 1995. Proceedings., IEEE International Conference on*, vol. 4, pp. 1942–1948 vol.4.

[12] Yang and Xin-She, *Engineering optimization: An introduction with metaheuristic application*. Hoboken: John Wiley, 2010.

[13] Y. del Valle, G. K. Venayagamoorthy, S. Mohagheghi, J. C. Hernandez, and R. G. Harley, "Particle swarm optimization: Basic concepts, variants and applications in power systems," *Evolutionary Computation, IEEE Transactions on*, vol. 12, no. 2, pp. 171–195, 2008.

[14] D. Maiti, A. Acharya, M. Chakraborty, A. Konar, and R. Janarthanan, "Tuning pid controllers using the integral time absolute error criterion," in *Information and Automation for Sustainability, 2008. ICIAFS 2008. 4th International Conference on*, pp. 457–462.

[15] "Ieee standard for interconnecting distributed resources with electric power systems," *IEEE Std 1547-2003*, 2003.